ՀՀ ԳԱԱ Վ. Հ. ՀԱՄԲԱՐՁՈՒՄՅԱՆԻ ԱՆՎԱՆ ԲՅՈՒՐԱԿԱՆԻ ԱՍՏՂԱԴԻՏԱՐԱՆ

ՆԱԻՐԱ ՄՈՒՇԵՂԻ ԱԶԱՏՅԱՆ

«Երիտասարդ ենթակարմիր աստղակույտերի որոնում և ուսումնասիրություն»

Ա.03.02 – «Աստղաֆիզիկա, ռադիոաստղագիտություն» մասնագիտությամբ ֆիզիկամաթեմատիկական գիտությունների թեկնածուի գիտական աստիճանի հայցման ատենախոսության

ՍԵՂՄԱԳԻՐ

Բյուրական-2022

NAS RA BYURAKAN ASTROPHYSICAL OBSERVATORY AFTER V. A. AMBARTSUMIAN

NAIRA M. AZATYAN

«Search and study of young infrared stellar clusters»

Thesis for the degree of candidate in physical and mathematical sciences

Specialty 01.03.02 – “Astrophysics and Radioastronomy”

SYNOPSIS

Byurakan–2022

Ատենախոսության թեման հաստատվել է ՀՀ ԳԱԱ Վ. Համբարձումյանի անվան Բյուրականի աստղադիտարանի գիտական խորհրդում

Գիտական ղեկավար՝
ֆիզ.-մաթ. գիտ. թեկնածու Ելենա Նիկողոսյան

Պաշտոնական ընդդիմախոսներ՝
ֆիզ.-մաթ. գիտ. դոկտոր Գագիկ Տեր-Ղազարյան
ֆիզ.-մաթ. գիտ. թեկնածու Մեխակ Հայրապետյան

Առաջատար կազմակերպություն՝
Ռուսաստանի գիտությունների ակադեմիայի աստղագիտության ինստիտուտ (INASAN)

Պաշտպանությունը կայանալու է 2022 թ. նոյեմբերի 17-ին ժամը 14:00-ին, ՀՀ ԳԱԱ Վ. Համբարձումյանի անվան Բյուրականի աստղադիտարանում, 048 մասնագիտական խորհրդում:

Ատենախոսությանը կարելի է ծանոթանալ ՀՀ ԳԱԱ Վ. Համբարձումյանի անվան Բյուրականի աստղադիտարանում

Սեղմագիրը առաքված է 2022 թ. սեպտեմբերի 28-ին:

Մասնագիտական խորհրդի գիտական քարտուղար՝  ֆիզ.-մաթ. գիտ. թեկնածու Ելենա Նիկողոսյան

The thesis theme is approved by the scientific council of the NAS RA Byurakan Astrophysical Observatory after V. A. Ambartsumian

Scientific advisor:
Candidate of Phys. Math. Sciences Elena Nikoghosyan

Official opponents:
Doctor of Phys. Math. Sciences Gagik Ter-Kazarian
Candidate of Phys. Math. Sciences Mekhak Hayrapetyan

Leading Organization:
Institute of Astronomy of the Russian Academy of Sciences (INASAN)

The defense of the thesis will take place at 14:00 on 17 November 2022 on the session of the Special Council 048 of the NAS RA Byurakan Astrophysical Observatory after V. A. Ambartsumian

The thesis is available in the library of NAS RA Byurakan Astrophysical Observatory after V. A. Ambartsumian.

The synopsis is distributed on 28 September 2022.

Scientific secretary of the Special Council  Candidate of Phys. Math. Sciences Elena Nikoghosyan

GENRAL DESCRIPTION OF THE THESIS

Relevance of the topic

The star formation process continues at all stages of the evolution of our and other galaxies, including the present stage [1], and is one of the most important processes which provides the observational output of the galaxies. The evolutionary process of stars enriches the surrounding environment by heavy elements through a continuous manner via powerful stellar winds and an instantaneous manner via supernova explosions accompanied by a strong release of energy, which, in addition to generating turbulent motions in the surrounding gas-dust matter, contributes to maintaining its highly heterogeneous structure and may, under certain circumstances, give birth to new molecular regions prone to star formation. Therefore, young stellar clusters are recognized as important tracers of recent star formation in galaxies and of spiral structure in galactic disks with a wide range of stellar masses (from O high-mass stellar objects to brown dwarfs) within relativity small volume of space. Since stars in such groups have the common heritage of being formed more or less simultaneously from the same progenitor molecular cloud, observations of a cluster can be used to provide classical tests of stellar evolution theory. There is a large number of observation data, which witness that the star formation process has consecutive nature [9]. Therefore, the spatial distribution of young stellar objects (YSOs) in clusters and the quantitative ratio between YSOs with different masses and ages are essential for understanding the evolutionary history of a cluster itself. However, such studies have been seriously hampered by the fact that galactic clusters form in giant molecular clouds and during their formation and earliest stages of evolution are completely embedded in molecular gas and dust, and thus obscured from view. Given the constraints imposed by traditional techniques of optical astronomy, direct observation and study of young embedded clusters had been extremely difficult, if not impossible. However, during the last two decades, the development of infrared (IR) astronomy has dramatically improved this situation providing astronomers the ability to survey and systematically study embedded clusters within molecular clouds.

Embedded stellar clusters, which are still surrounded by molecular clouds are of particular interest to understand which properties of stellar clusters are related to their origins and which are derived from subsequent evolution. There is also a certain relationship between the properties of the stellar population of young clusters and the process of their formation. If the star-formation in clusters is triggered, the age spread of stars in the cluster should be small, while in self-initiated protocluster condensations, the individual clumps should have a larger age spread [11].

Investigations have shown that more than one mechanism may be at work forming clusters in the natal molecular cloud and in most cases embedded clusters are associated with IRAS sources [6]. The obtained data only strengthened the confidence that

stars are born in deeply embedded regions, which contain a significant amount of intimately mixed relatively cold gas and dust [7] which is called the interstellar medium (ISM). The matter in ISM manifests itself primarily through obscuration, reddening, and polarization of starlight, through the formation of absorption lines in stellar spectra, and through various emission mechanisms (~10–15% of the total mass of the Galactic disk). It tends to concentrate near the Galactic plane and along the spiral arms while being very inhomogeneously distributed at small scales. It displays dramatic density and temperature contrasts, such that only the densest, coldest molecular regions can offer an environment favorable to star formation [3]. Consequently, the study of ISM in conjunction with the study of embedded in them YSOs is very important for understanding the process of formation and evolution of the stellar population.

Despite all efforts, however, today there are much more questions in the theory of star formation than answers to them. Some of the relatively clarified questions include the mechanism of low-mass star formation. The formation of low-mass TTau stars is composed of different stages. These theoretical stages have been confirmed by observations of stellar objects at different evolutionary stages: from molecular protostellar clouds to low-mass main-sequence stars. Several studies show that most intermediate-mass Herbig Ae/Be stars share a number of characteristics of low-mass stars [4]. However, extending this theory to high-mass stars is not trivial. One of the many reasons is that high dust extinction makes it difficult to observe high-mass stars during critical early formation phases. They evolve quickly and important evolutionary phases are short-lived. As a result, high-mass stars reach the zero-age main sequence (ZAMS) while still accreting (e.g. [5]).

The aim of the thesis

The thesis is devoted to the investigation of the star-forming regions analyzing a large amount of IR data. In particular, the aims are:

- The search for young stellar clusters in the vicinity of IRAS objects, which appear to be associated with high-mass YSOs;
- Identification of the clusters' members using their IR properties;
- Investigation of structural properties of young stellar clusters;
- Determination of age and age spread of clusters' members;
- Construction of the Luminocity Functions (LFs) and Mass Functions (MFs) for clusters;
- Determination of ISM parameters, namely the distribution of hydrogen column density ($N(H_2)$) and dust temperature (T_d);
- Determination of the star formation efficiency (SFE) and star formation rate (SFR)

Scientific novelty

In this thesis novel approach is used for data analysis which includes the combination of different methods. Young compact clusters have been discovered around 16 out of the 20 IRAS sources, including 4 for the first time. For a more detailed study, 3 clusters (IRAS 05137+3919, 05168+3634 and 19110+1045) were selected with presumably different stellar populations. In these star-forming regions the physical parameters of the ISM are estimated and rich population of embedded YSOs are identified and investigated. The results show the direct relationship between surface stellar density and hydrogen column density in all three star-forming regions. The distribution of identified YSOs shows that Class I sources are mostly found in the detected dense clusters, while Class II have a wider distribution.

Studying common structure of the molecular cloud surrounding IRAS 05168+3634, it turns out that apart from it, there are four IRAS sources (IRAS 05184+3635, 05177+3636, 05162+3639, and 05156+3643) embedded in the same molecular cloud.

The age of the IRAS 05137+3919 and 05168+3634 star-forming regions is estimated to be between 0.1 and 3 Myr, while the age of the physically connected IRAS 19110+1045 and 19111+1048 (or G45.12+0.13 and G45.07+0.13 UCHII regions) star formation regions is 1 Myr. This suggests that star formation in the first two star-forming regions started as a result of the independent condensation of their molecular clouds, while in IRAS 19110+1045 and 19111+1048 star-forming regions - as a result of the triggering shock.

Practical importance

The thesis may contribute to the star formation theory which is one of the most important problems in the modern astrophysics. The introduced innovative methods can be used to investigate other star-forming regions because the obtained results are highly reliable.

Obtained results in the G45.12+0.13 and G45.07+0.13 UCHII regions can be strong confirmation of triggered star formation and very good starts for investigation of massive star formation in the GRSMC 45.46+0.05 molecular cloud since it contains a number of other UCHII regions and, therefore, high-mass stars.

Basic results to be defended:

1. At least for 20 regions, we obtained that around a middle- and high-mass YSO, in a certain stage of evolution, a group of young stars was formed and with modified selection criteria (depth of images, longer wavelength range), the percentage of detected groups should increase.
2. The selected YSOs are distributed nonuniformly in the IRAS05137+3919 star-forming region and form two subgroups.
3. The distribution of stars in the IRAS05168+3634 field made it possible to reveal five dense subgroups around IRAS sources, which repeat the shape of the

molecular cloud seen in far-infrared (FIR) wavelengths. We concluded that IRAS05168+3634 and other four sub-regions (IRAS 05184+3635, 05177+3636, 05162+3639, and 05156+3643) are embedded in the single molecular cloud and based on *Gaia* EDR3 parallaxes are located at ~1.9 kpc distance.

4. The age spread of the IRAS05137+3919 and IRAS05168+3634 star-forming regions is much larger, and, therefore, it can be concluded that the stellar population is formed as a result of independent condensations in the parent molecular cloud.
5. The presence of a region (bridge) with relatively high density and low temperature positioned between the G45.12+0.13 and G45.07+0.13 UCHII regions suggests that these UCHII regions are physically connected.
6. Based on the data obtained by the SED fitting tool, the minimum and maximum estimated mass in the region surrounding IRAS 19110+1045 and 19111+1048 are 1.7 and 22 $M_{\odot}$, respectively.
7. We presumed that the low-density extended emission observed on the MIR images, which also stands out well on the dust temperature maps in G45.12+0.13 and G45.07+0.13 UCHII regions, may be due to the existence of the stellar clusters.
8. The IRAS clusters' members in G45.12+0.13 and G45.07+0.13 UCHII regions exhibit low scatter relative to the isochrones and their evolutionary age distribution shows small spread. Therefore, we concluded that their origin can be relate to an external triggering shock.
9. We assumed that uniformly distributed non-cluster YSOs in the region surrounding IRAS 19110+1045 and 19111+1048 are part of the young stellar population of the GRSMC 45.46+0.05 molecular cloud.
10. The distribution of classified YSOs in the field showed that Class II objects are distributed more homogeneously on the field than Class I objects, which are located in certain areas and show clear concentrations. This confirms the assumption that, unlike the Class II objects, Class I objects did not have enough time to leave their birthplaces after formation.

Approbation of the work:

The main results of the thesis had been presented in the following conferences:

1. Armenian-Iranian Astronomical Workshop, 13-16 October, 2015, Byurakan, Armenia
2. Star Cluster: From Infancy to Teenagehood, 8-12 August, 2016, Heidelberg, Germany
3. Non-Stable Universe: Energetic Resources, Activity Phenomena and Evolutionary Processes, 19-23 September 2016 in Yerevan and Byurakan, Armenia

4. Stellar Associations: 70 Years of Research, 25-27 September, 2017, Byurakan, Armenia
5. The Olympian Symposium 2018 "Gas and stars from milli- to mega- parsecs", 28 May – 1 June 2018, Paralia Katerini, Mount Olympus, Greece.
6. Instability Phenomena and Evolution of the Universe, 17.09-21.09, 2018, Byurakan, Armenia
7. Astronomical Surveys and Big Data 2, 14-18 September, 2020, Byurakan, Armenia
8. European Astronomical Society Annual Meeting 2021, 28 June – 2 July, 2021, Virtual meeting
9. Astronomy in the Crossroads of Interdisciplinary and Multidisciplinary Sciences, 22-25 September, 2021, Virtual meeting
10. Joint International Conference on Astrophysics for Young Scientists, 14-15 October, 2021, Virtual meeting
11. From Stars to Galaxies II, 20-24 June 2022, Chalmers University, Gothenburg, Sweden
12. European Astronomical Society Annual Meeting 2022, 27 June - 1 July 2022, Valencia, Spain
13. International Astronomical Union General Assembly 2022, 2-11 August 2022, Busan, Republic of Korea

Structure of the thesis

The thesis consists of five chapters including Introduction and main Conclusions and References. The thesis contains 131 pages, including 37 figures and 19 tables (6 long tables are online).

Content of the thesis

In **Introduction (Chapter 1)**, the current state of the star formation theory is presented emphasizing the role of star clusters (and ISM) in that process. Unsolved questions related to star formation are also reviewed. The structure, publications in the topic and aims of the thesis are presented.

In **Chapter 2**, the used data and methods are described. This chapter contains three sub-sections. In the first sub-section, we described the used observational data, which are covering a wide range of near-infrared (NIR) to FIR. The thesis contains two main scientific directions, namely study of ISM and YSOs. To study gas and dust, as well as deeply embedded point sources, we used FIR observations in the 70–500 μm range since this wavelength range covers the peak of the spectral energy distribution of cold dust emission. Modified single-temperature blackbody fitting was subsequently carried out to obtain the important ISM parameters such as the hydrogen column density ($N(H_2)$) and the dust temperature (T_d). To select and study the potential stellar members of the star-

forming regions, we used NIR, mid-infrared (MIR), and FIR data. Since, the presence of circumstellar discs and envelopes cause an IR excess of a YSO, therefore YSO candidates were identified based on their position in colour–colour (c-c) infrared diagrams. The choice of colours depends on the available data. The selection criterion does not, of course, give us very complete list of the clusters' members. To confirm the selected YSOs and to determine their parameters, we constructed their SEDs and fitted them with the radiative transfer models of [8].

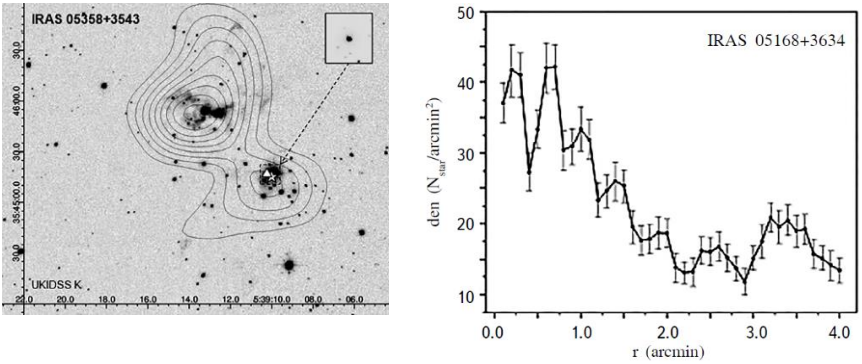

Figure 1. *(Left)* NIR images and isodenses of IRAS05358+3543 star-forming region. IRAS and MSX sources are indicated by stars and triangles, respectively. *(Right)* Radial distribution of the stellar density relative to IRAS05168+3634 source. Vertical lines are standard errors.

In **Chapter 3**, the results of the search and study of compact clusters in 20 star-forming regions are presented. In order to detect clusters in considered 20 regions, we constructed surface stellar density distribution maps around each IRAS source using NIR and MIR photometric data. To confirm the results of surface stellar density distribution maps and to refine the sizes of existing clusters, we also constructed the radial density distribution of stars with respect to the geometric center of the group. Figure 1 shows the examples of surface stellar density distribution map (left panel) and radial density distribution of stars (right panel) in two different star-forming regions. We have also compared the LF of stellar objects in the clusters and their fields using the Kolmogorov-Smirnov test. We were able to detect compact clusters in 12 and 4 regions based on NIR and MIR data, respectively. This represents 80% of the overall number of regions that were studied and is substantially higher than the results based on data from the Two Micron Sky Survey (2MASS). This chapter also contains short descriptions of considered 20 star-forming regions and parameters of their central YSOs. At least for these 20 regions, we concluded that around middle- and high-mass YSO, in a certain stage of evolution, a

group of young stars was formed and with modified selection criteria (depth of images, longer wavelength range), the percentage of detected groups should increase.

In **Chapter 4**, a detailed study of three star-forming regions, namely IRAS 05137+3919, 05168+3634, and 19110+1045 is presented, which includes the study of both the stellar population and the ISM. The main selection criteria of these three regions are their considerable extent and multicomponent complex structure, which implies the presence of several local nests of star formation. The regions are little studied, but at the same time, there is sufficient observational data for their detailed study. Besides, our preliminary studies have shown that the star-forming regions differ in their stellar composition and structural properties. These star-forming regions are also of interest because they are located at large distances, which will allow us to test the capabilities of the databases at our disposal. All three regions, despite their certain differences, are united by one aspect - they are regions of active star formation. This chapter contains 3 main sub-sections and each sub-section describe the detailed study of the star-forming regions.

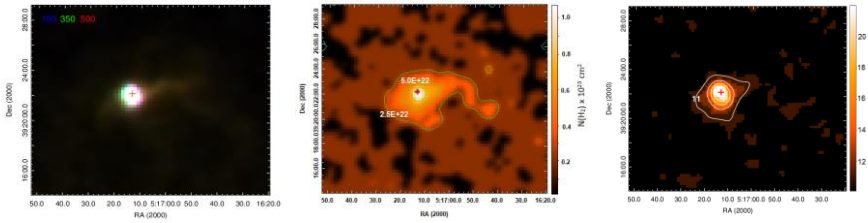

Figure 2. (*Left*) Colour-composite image of IRAS05137+3919 star-forming region: 160 μm (blue), 350 μm (green), and 500 μm (red). (*Middle*) Column density map of the region. The external isodense corresponds to the 2.5x10^{22} cm^{-2} value and the interval between isodences is also 2.5x10^{22} cm^{-2}. (*Right*) Dust temperature of the region. The external isotherm corresponds to 11 K and interval between isotherms is 2.5 K. The position of the IRAS source is indicated by red cross.

The first sub-section presents the investigation results of a young stellar cluster located in the vicinity of IRAS05137+3919 associated with the CPM 15 YSO. Different manifestations of active star formation have been observed in this region, such as maser emissions, as well as CO and H_2 outflows. Left panel of Figure **2** shows the colour-composite image covering the IRAS05137+3919 star-forming region. The region stands out sharply in terms of brightness. Using the modified single-temperature blackbody fitting, we have determined the main parameters ($N(H_2)$ and T_d) of cold composing gas-dust matter in the region and their maps are presented in the middle and right panels of Figure **2**. The $N(H_2)$ and T_d maps show that the star-forming region stands out sharply in terms of brightness with a relatively high density and temperature. The maxima of both

$N(H_2)$ (~$1.0x10^{23}$ cm^{-2}) and T_d (22 K) almost coincide with position of the IRAS source. Towards the periphery, both parameters decrease up to $2.2x10^{22}$ cm^{-2} and 11 K.

The radial distribution of stars density relative to the position of IRAS05137+3919 confirmed the existence of a cluster in the vicinity of the IRAS source with 1.5′ radius. Within this radius, the stellar density (38 stars/arcmin^2) is twice the density of the field (19 stars/arcmin^2).

The selection of YSOs in the IRAS05137+3919 star-forming region was based on two c-c diagrams, namely (J-H) versus (H-K) and (J-K) versus [3.6]-[4.5]. Figure **3** (left and right panels) shows the positions of 253 objects located within 1.5′ radius relative to the IRAS05137+3919 source. Totally, we selected 84 YSOs (blue circles) based on these two c-c diagrams. This is almost 1.5 times greater than the earlier estimate of the cluster members [2]. Since stellar magnitudes in the *Spitzer* 3.6 and 4.5 μm bands are available for only 33 YSOs, we were able to obtain parameters of these YSOs using the SED fitting tool. The full tables of selected YSOs with their parameters are included in the thesis. The selected YSOs are distributed nonuniformly in the star-forming region and form two subgroups; one is located around CPM 15, while the second group contains a significant number of middle-mass objects surrounded by gas-dust nebulae.

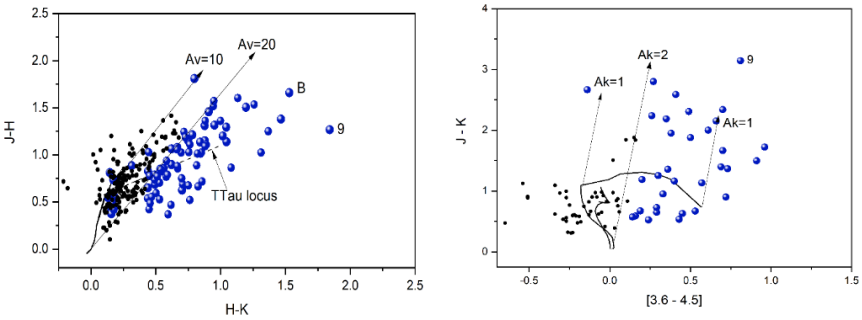

Figure 3. (*Left*) (J-H) vs. (H-K) and (*Right*) (J-K) vs. [3.6]-[4.5] c-c diagrams for IRAS05137+3919 star-forming region. Not all non-classified objects (black circles) are presented in these diagrams. Southwest component B of CPM15 YSO and the reddest object with number 9 are labeled.

The distribution of 33 identified YSOs in colour-magnitude diagram (CMD) and histograms of their evolutionary ages clearly showed very wide spread. On the basis of these, it can be assumed that, in general, the star formation process in the considered region is sequential. In addition, based on K luminosity function (KLF) slope, the age of IRAS05137+3919 star-forming region is estimated between 0.1 and 3 Myr. Therefore, the large age spread of IRAS05137+3919 star-forming region give us bases to conclude that

the stellar population is formed as a result of independent condensations in the parent molecular cloud.

The second sub-section presents the investigation results of a young stellar cluster located in the vicinity of IRAS05168+3634 source. The presence of different maser emissions and ^{13}CO cores confirms its active star-forming nature. The region has a more complicated structure in the FIR wavelengths than in the NIR (see Figure **4**). The complex structure of the region is clearly visible in FIR (right panel). Moving toward longer wavelengths, the cloud filaments surrounding IRAS05168+3634 become more visible and it is obvious that the IRAS05168+3634 star-forming region is more extended and is located within a 24 arcmin radius molecular cloud. Studying the common star-forming region in the molecular cloud, it turns out that apart from IRAS05168+3634, there are four IRAS sources (IRAS 05184+3635, 05177+3636, 05162+3639, and 05156+3643) embedded in the same molecular cloud. Since, the distribution of stars in our field is 35 times different from the homogeneous distribution and their distribution in the field repeats the shape of the molecular cloud seen in FIR wavelengths, we concluded with a high probability that all five IRAS star-forming regions are at the same distance.

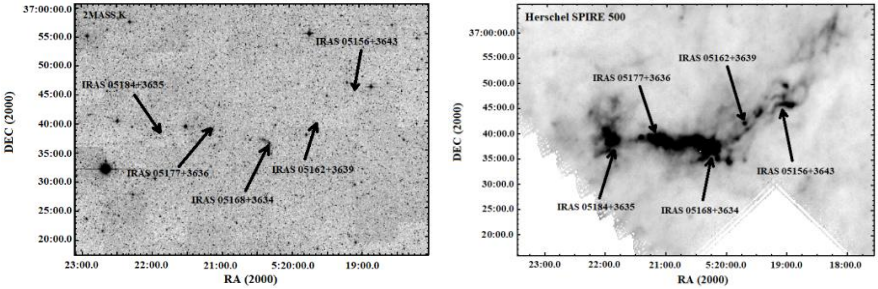

Figure 4. The IRAS05138+3634 star-forming region at (*left*) NIR (2MASS K-band) and (*right*) FIR (*Herschel* SPIRE 500 μm) wavelength ranges. The positions of five IRAS sources are indicated by arrows.

The $N(H_2)$ and T_d maps in the left and right panels of Figure **5** show that the star-forming region clearly stands out against the background of the surrounding molecular cloud both with a higher density and temperature. The relatively hotter gas-dusty matter forms dense condensations around IRAS objects. An exception is the IRAS05162+3639 sub-region, near which on the $N(H_2)$ map there is practically no region with a relatively higher density and no group of YSOs has been identified around this source, but only 5 stars. In general, in the whole star-forming region T_d varies from 11 to 24 K, and $N(H_2)$ - from ~1.0 to 4.0x10^{23} cm^{-2}.

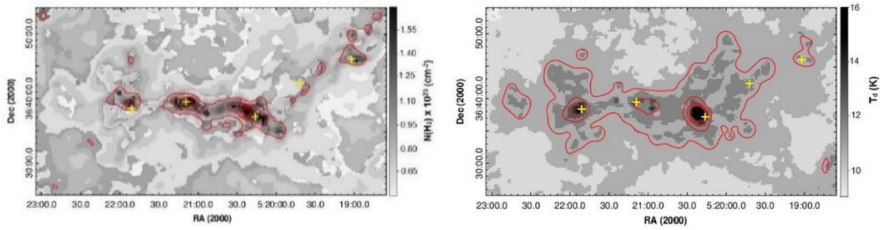

Figure 5. Maps of $N(H_2)$ column density (*left*) and T_d dust temperature (*right*) of IRAS05168+3634 star-forming region. The outer isodense on the $N(H_2)$ map corresponds to $0.9x10^{23}$ cm^{-2}, and the interval between isodenses is $\sim 0.4x10^{23}$ cm^{-2}. The outer isotherm on the T_d map corresponds to 11 K, and the interval between isotherms is 1 K. The positions of IRAS sources are marked by yellow crosses.

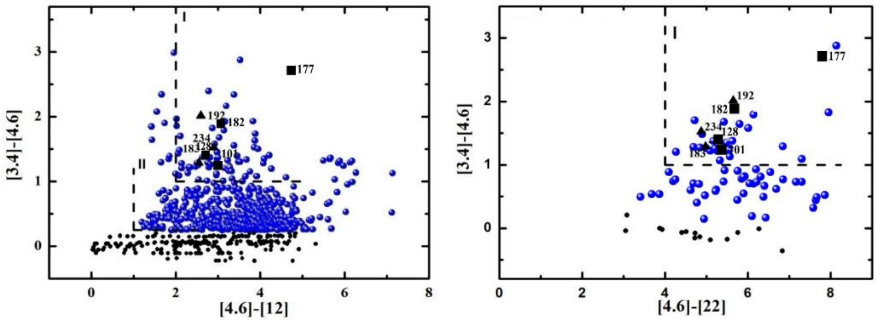

Figure 6. [3.4]–[4.6] vs. [4.6]–[12] (*left*) and [3.4]–[4.6] vs. [4.6]–[22] (*right*) c-c diagrams for the IRAS05168+3634 star-forming region. The blue circles are selected YSOs and black circles are unclassified ones. Not all unclassified objects are presented in these diagrams. IRAS and MSX sources are indicated by triangles and squares, respectively, and they are labeled.

The selection of YSOs in the IRAS05168+3634 star-forming region was based on four c-c diagrams, namely (J-H) versus (H-K), K-[3.6] versus [3.6]-[4.5], [3.4]-[4.6] versus [4.6]-[12], and [3.4]-[4.6] versus [4.6]-[22]. Figure 6 shows only two of these c-c diagrams. We added to our list those objects classified as YSOs in at least two c-c diagrams. Totally, we selected 1224 YSOs within a 24 arcmin radius. The distribution of classified YSOs in the field showed that Class II objects are distributed more homogeneously on the field than Class I objects, which are located in certain areas and show clear concentrations with sub-structures. This confirms the assumption that, unlike the Class II objects, Class I objects did not have enough time to leave their birthplaces after formation. Since the region is quite large, further investigations have only been performed on concentration

areas. We estimated the size of each concentration in the molecular cloud based on map of the distribution of stellar surface density. Then, 240 YSOs of 1224 selected from c-c diagrams within the determined radii were explored in greater detail. The full tables of 240 selected YSOs with their NIR, MIR and FIR photometry and parameters (only 120 YSOs) obtained by SED fitting tool are available VizieR On-line Data Catalog[1].

The distribution of selected YSOs in K versus J-K CMDs and histograms of their evolutionary ages clearly showed very wide spread as in IRAS05137+3919 case. KLF slopes suggested that the age of all four subregions (except IRAS05162+3639) can be estimated between 0.1 and 3 Myr. In the case of the IRAS05162+3639 subregion, there are not enough YSOs to construct the KLF. Therefore, the large age spread of IRAS05168+3634 star-forming region give us bases to conclude that the stellar population is formed as a result of independent condensations in the parent molecular cloud.

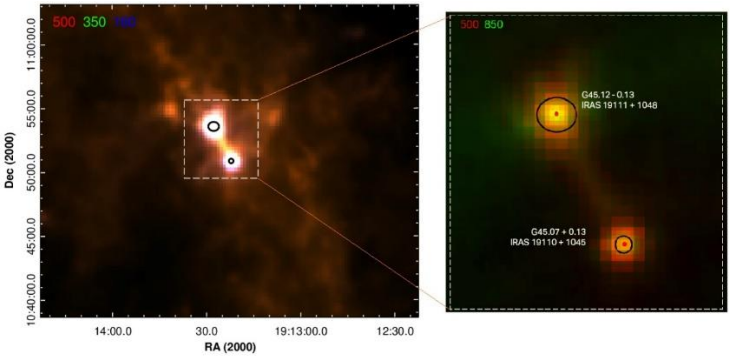

Figure 7. Colour-composite images of G45.12+0.13 and G45.07+0.13 UCHII regions. Left panel: *Herschel* 160 μm (blue), 350 μm (green), and 500 μm (red); right panel: zoomed area (white dotted square) at SCUBA 850 μm (green) and *Herschel* 500 μm (red). The positions and dimensions of the radio sources are marked by black circles. A red dot represents the position of an IRAS source.

Since, the results for the distance of IRAS05168+3634 star-forming region are quite different (1.88 and 6.1 kpc), we attempt to identify the list of YSOs in the *Gaia* EDR3 database. In total, we were able to identify 65 objects, but only for 11 of them (located in all five sub-regions) the parallax measurement accuracy is high enough ($\varpi/\sigma_{\varpi} > 5$) and such a small number of objects is quite expected since YSOs are embedded in a dense ISM. The result obtained from *Gaia* EDR3 data can be considered as one more argument in favor

[1]The full tables are available in VizieR On-line Data Catalog: J/A+A/622/A38

of the fact that all sub-regions are embedded in the single molecular cloud and belong to the same star-forming region, which is located at ~1.9 kpc distance.

The last sub-section presents the investigation results of star-forming regions associated with IRAS 19110+1045 and 19111+1048 sources, referred to as G45.07+0.13 and G45.12+0.13 UCHII regions, respectively. This complex is an ideal laboratory to investigate the early stages of massive star formations and their influence on natal environments. Figure 7 presents colour-composite images covering the molecular cloud. The G45.12+0.13 and G45.07+0.13 UCHII regions stand out sharply in terms of brightness. The images also indicate that the UCHII regions are connected by a relatively colder bridge and are thus very likely a physically bound system.

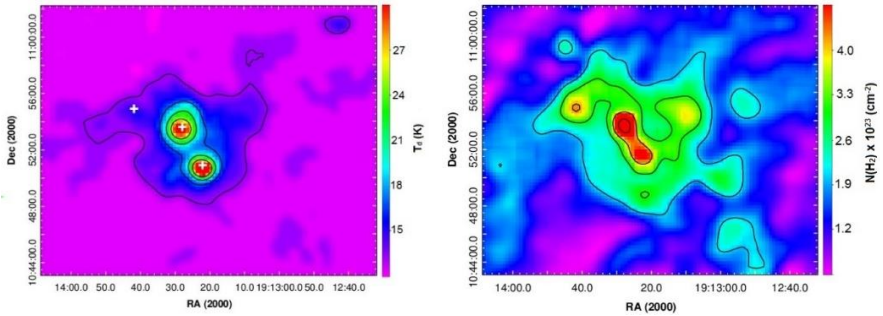

Figure 8. Maps of T_d dust temperature (*left*) and N(H_2) column density (*right*) of the region surrounding G45.12+0.13 and G45.07+0.13 UCHII objects. The outer isotherm corresponds to 13 K and the interval between isotherms is 4 K. The outer isodense corresponds to 2.0×10^{23} cm^{-2} and interval between isodenses is 1.0×10^{23} cm^{-2}. The positions of the IRAS and BGPC 6737 sources are marked by white crosses.

The N(H_2) and T_d maps of the wider region surrounding the G45.12+0.13 and G45.07+0.13 UCHII objects are shown in Figure 8. Both UCHII regions are distinct from the molecular cloud due to their high dust temperature and column density with an almost spherically symmetric distribution. This is fully consistent with the basic concept of UCHII regions about the presence of a hot, high mass stellar source and stellar wind, which leads to the blowing out of matter [10]. In general, within both regions, T_d varies from about 17 to 40 K and N(H_2) varies from about 3.0×10^{23} to 5.5×10^{23} cm^{-2}. T_d drops significantly from the centres to the periphery, reaching a value of about 18–20 K. In G45.07+0.13 region, the IRAS source is somewhat offset from the density maximum. Near IRAS19110+1045, the column density is ~3.5×10^{23} cm^{-2}. The IRAS source is located close to the dust temperature maximum (T_d = 42 K). In G45.12+0.13 region, the position of IRAS19111+1048 coincides with the maxima of both the column density (5.5×10^{23} cm^{-2}) and temperature (35 K). The isotherms are slightly elongated towards the northwest,

which may relate to the presence of two UCHIIs (G45.12+0.13 and G45.13+0.14). The presence of a region (bridge) with relatively high density ($N(H_2)\approx 4.3x10^{23}$ cm^{-2}) and low temperature (T_d ≈19 K) positioned between the two UCHII regions suggests that they are physically connected.

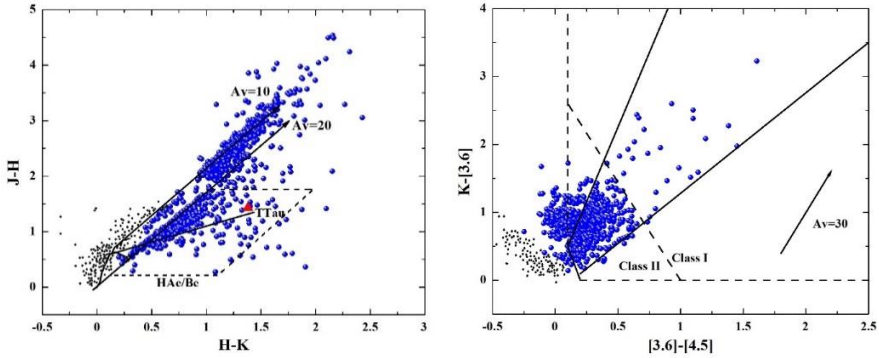

Figure 9. (J-H) vs. (H-K) (*left*) and K-[3.6] vs. [3.6]-[4.5] (*right*) c-c diagrams of the IRAS 19110+1045 and 19111+1048 star-forming regions. The blue circles are selected YSO candidates and black circles are non-classified ones. Not all non-classified objects are presented in these diagrams. IRAS19111+1048 source is indicated by a red triangle.

The selection of YSOs in the IRAS 19110+1045 and 19111+1048 star-forming regions was based on six c-c diagrams, namely (J-H) versus (H-K), K-[3.6] versus [3.6]-[4.5], [3.6]-[4.5] versus [5.8]-[8.0], [3.6]-[5.8] versus [8.0]-[24], [3.4]-[4.6] versus [4.6]-[12], and [3.4]-[4.6] versus [4.6]-[22]. Figure 9 shows only two of these c-c diagrams. We added to our list those objects classified as YSOs in at least two c-c diagrams. However, since the region has two saturated areas in the MIR band around the IRAS sources (IRAS19110+1045 with 25″ radius and IRAS19111+1048 with 50″ radius), objects within those areas classified as YSOs based on only the NIR c-c diagram were included in the list of YSO candidates. We selected 909 YSOs within a 6 arcmin radius. Excluding objects in two MIR–saturated regions (115 YSOs), we achieved relatively robust parameters for 431 of the 793 selected YSOs. We also performed a visual inspection of the YSO candidates in two MIR–saturated regions, because from our point of view, these objects are of the greatest interest as they are located in the immediate vicinity of the UCHIIs. Overall, the final list comprised 518 YSOs (423 with constructed SEDs and 95 YSOs in two saturated regions). The full tables of 518 selected YSOs with their NIR, MIR and FIR photometry and parameters obtained by SED fitting tool are available VizieR On-line Data Catalog[2].

[2] The full table is available in VizieR On-line Data Catalog: J/other/PASA/39.24

The selected YSOs form dense clusters in both UCHII regions. Therefore, the low-density extended emission observed on the MIR images, which also stands out well on the dust temperature maps in both UCHII regions, may be due to the existence of the stellar clusters. Based on the data obtained by the SED fitting tool, the minimum and maximum estimated mass in the region is 1.7 and 22 $M_{\odot}$, respectively. Primarily, the lack of low-mass stellar objects can be explained by the large distance of the star-forming region. We were able to identify NIR counterpart of IRAS19111+1048 source, which has 9.4±4.3 $M_{\odot}$ mass, 23 000±11 000 K temperature, and (2.5±1.2)x10^6 years evolutionary age. Unfortunately, due to the saturation of the central parts of the UCHII regions in the MIR range, we were unable to identify the YSOs associated with IRAS19110+1045 source.

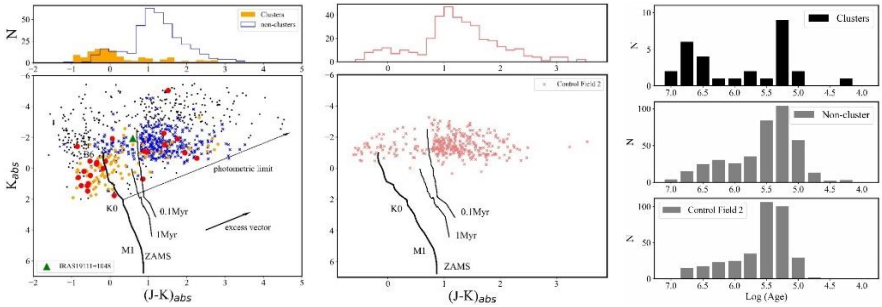

Figure 10. (*Bottom left and middle*) K versus (J–K) CMDs for identified YSOs in the IRAS 19110+1045 and 19111+1048 star-forming regions, and Control field 2, respectively. Red circles are stellar objects within the IRAS clusters with constructed SED. Objects located in the saturated regions are yellow circles. Non-cluster objects are blue crosses and no-SED objects are black dots. IRAS19111+1048 source is indicated by a green triangle and labelled. Stellar objects located in Control field 2 are indicated by coral crosses. (*Top left and middle*) Histograms of $(J-K)_{abs}$ values. (*Right*) Histogram of evolutionary ages for members of the IRAS clusters (*top*), the non-cluster objects (*middle*), and the objects in the Control field 2 (*bottom*).

The distribution of the identified YSOs in the K versus J–K CMD is shown in the left and middle panels of Figure 10. The positions of objects in the two IRAS clusters (circles) and non-cluster objects (crosses) are different. The clusters' members and non-cluster objects exhibit low scatter relative to the isochrones. An overwhelming majority (more than 80%) of the non-cluster objects are younger than 0.1 Myr. In contrast, about 75% of objects in the IRAS clusters are older than 0.1 Myr and concentrated around the ZAMS. For improved clarity, the histograms of $(J-K)_{abs}$ are shown in the top left and middle panels. In general, the $(J-K)_{abs}$ spread of the vast majority of stellar objects from both samples is small. The distribution of evolutionary ages (by the SED fitting tool) for

the non-cluster (middle right) and Control field 2 (lower right) objects has a well-defined, coincident peak and confirms the results of $(J-K)_{abs}$ histograms. In contrast, the distribution of the evolutionary ages of the objects in the clusters has two peaks (top right) which was constructed based on parameters from only 29 YSOs for which the SED fitting tool was applied. Most of the other 95 YSOs in the MIR-saturated regions are concentrated around the ZAMS and to the left of the 1 Myr isochrone. Therefore, we assumed that these objects will have a real contribution to the first peak in the evolutionary age distribution. Accordingly, this distribution will have only one well-defined peak as the histogram of $(J-K)_{abs}$. The small spread of evolutionary ages suggests that the clusters owe their origin to a triggering shock.

The non-cluster YSOs are found to be uniformly distributed in the molecular cloud. Therefore, the origin of the non-cluster objects cannot be explained by the activity of the embedded massive stars in the UCHII regions. To understand the existence of the non-cluster objects, we performed the same analysis in Control field 2 which is very close to the considered region. YSOs in Control field 2 show the same behavior as the non-cluster objects (evolutionary ages, masses, and surface stellar density). Accordingly, it is plausible that the non-cluster YSOs are part of the young stellar population of the GRSMC 45.46+0.05 molecular cloud. To understand the tracers of their origins, the star formation history of the GRSMC 45.46+0.05 star-forming region as a whole must be investigated.

In **Conclusions (Chapter 5)**, the main results of the thesis are presented.

Publications in the topic of thesis

1. Nikoghosyan E. and **Azatyan N.**, "*Young Stellar Cluster in the Vicinity of the IRAS 05137+3919 Source*" Astrophysics, 2014, 57, pp. 330-343
2. **Azatyan N. M.,** Nikoghosyan E. H., and Khachatryan K. G., "*Search for Compact Stellar Groups in the Vicinity of Iras Sources*" Astrophysics, 2016, 59, pp. 339-353
3. **Azatyan N. M**. and Nikoghosyan E. H., "*Investigation of the stellar content in the IRAS 05168+3634 star-forming region*" ComBAO, 2018, 65, pp. 228-239
4. **Azatyan N. M.,** "*Investigation of the stellar content in the IRAS 05168+3634 star-forming region*" A&A, 2019, 22, pp. 22
5. Nikoghosyan E., **Azatyan N.,** Harutyunian H., Baghdasaryan D., and Andreasyan D., "*Properties of ISM in two star-forming regions*" ComBAO, 2020, 67, pp. 187-192
6. **Azatyan N.**, Nikoghosyan E., Harutyunian H., Baghdasaryan D., and Andreasyan D., "*Stellar population in two star-forming regions*" ComBAO, 2020, 67, pp. 211-218
7. Nikoghosyan E. H., **Azatyan N. M.,** Andreasyan D. H., and Baghdasaryan D. S., "*The structure of the IRAS05168+3634 star-forming region*" ApSS, 2021, 366, id.114

8. **Azatyan N.,** Nikoghosyan E., Harutyunian H., Baghdasaryan D., and Andreasyan D., "*Infrared study of the star-forming region associated with the UC HII regions G45.07+0.13 and G45.12+0.13*" PASA, 2022, 39, e024

References

[1] Ambartsumian V. A., "*The evolution of stars and astrophysics*" Armenian Acad. Sci., Erevan, U.S.S.R., 1947

[2] Faustini F., Molinari S., Testi L., and Brand J., "*Properties of stellar clusters around high-mass young stars*" A&A, 2009, 503, pp. 801-816

[3] Ferrière K., "*The interstellar environment of our galaxy*" RvMP, 2001, 73, pp. 1031-1066

[4] Hillenbrand L. A., Strom S. E., Vrba F. J., and Keene J., "*Herbig Ae/Be Stars: Intermediate-Mass Stars Surrounded by Massive Circumstellar Accretion Disks*" ApJ, 1992, 397, p. 613

[5] Keto E., "*The Formation of Massive Stars by Accretion through Trapped Hypercompact H II Regions*" ApJ, 2003, 599, pp. 1196-1206

[6] Phelps R. L. and Lada E. A., "*Spatial Distribution of Embedded Clusters in the Rosette Molecular Cloud: Implications for Cluster Formation*" ApJ, 1997, 477, pp. 176-182

[7] Reach W. T., Heiles C., and Bernard J.-P., "*Variations between Dust and Gas in the Diffuse Interstellar Medium*" ApJ, 2015, 811, pp. 14

[8] Robitaille T. P., Whitney B. A., Indebetouw R., and Wood K., "*Interpreting Spectral Energy Distributions from Young Stellar Objects. II. Fitting Observed SEDs Using a Large Grid of Precomputed Models*" ApJS, 2007, 169, pp. 328-352

[9] Soderblom D. R., "*The Ages of Stars*" ARA&A, 2010, 48, pp. 581-629

[10] Stahler S. W. and Palla F., "*The Formation of Stars*" 2004, pp. 865

[11] Zinnecker H., McCaughrean M. J., and Wilking B. A, "*The Initial Stellar Population*" University of Arizona Press, 1993, p. 429

ԱՄՓՈՓԱԳԻՐ

Ատենախոսությունը նվիրված է աստղառաջացման տիրույթների ուսումնասիրությանը, որը վերլուծում է մեծ քանակությամբ ինֆրակարմիր տվյալներ: Մասնավորապես, ատենախոսության նպատակներն են.

- IRAS օբյեկտների շուրջ երիտասարդ աստղակույտերի որոնում, որոնք կապված են մեծ զանգվածով Երիտասարդ Աստղային Օբյեկտների (YSO)-ների հետ;
- Աստղակույտերի անդամների նույնացում՝ օգտագործելով նրանց դրսևորած (դիտողական յուրահատկությունները) հատկությունները ինֆրակարմիր տիրույթում;
- Երիտասարդ աստղակույտերի կառուցվածքային հատկությունների ուսումնասիրություն;
- Աստղակույտերի անդամների տարիքները և տարիքի բաշխումը;
- Աստղակույտերի լուսատվության ֆունկցիաների (LFs) և զանգվածի ֆունկցիաների (MFs) կառուցում;
- Միջաստղային միջավայրի (ISM) պարամետրերի որոշում, մասնավորապես ջրածնի սյունակային խտության ($N(H_2)$) և փոշու ջերմաստիճանի (T_d) բաշխում:

Ատենախոսությունում ներկայացված է 20 IRAS աղբյուրների շուրջ աստղակույտերի որոնման և ուսումնասիրության արդյունքները: Ներկայացված է նաև երեք՝ IRAS 05137+3919, 05168+3634 և 19110+1045 աստղառաջացման տիրույթների մանրամասն ուսումնասիրություն, որը ներառում է ինչպես աստղային բնակչություն, այնպես էլ ISM: Այդ երեք տիրույթների ընտրության հիմնական չափանիշները դրանց զգալի տարածվածությունն ու բազմաբաղադրիչ բարդ կառուցվածքն է, որը ենթադրում է աստղառաջացման մի քանի տեղային օջախների առկայություն: Այս տիրույթները հետաքրքրություն են ներկայացնում, քանի որ դրանք գտնվում են մեծ հեռավորությունների վրա, ինչը մեզ թույլ կտա ստուգել մեր կողմից օգտագործված տվյալների բազաների հնարավորությունները: Արդյունքները ցույց են տալիս, որ բոլոր երեք աստղառաջացման տիրույթներում գոյություն ունի ուղիղ կապ աստղերի մակերևութային խտության և $N(H_2)$)-ի միջև:

Ստացվել են հետևյալ հիմնական արդյունքները.

- 20 IRAS աղբյուրներից 16-ի շուրջ հայտնաբերվել են երիտասարդ կոմպակտ աստղակույտեր, որոնցից 4-ը՝ առաջին անգամ: Սա կազմում է ուսումնասիրված տիրույթների ընդհանուր թվի 80%-ը և զգալիորեն ավելի բարձր է, քան երկու միկրո երկնքի շրջահայության (2MASS) տվյալների հիման վրա ստացված արդյունքները;
- Առնվազն 20 տիրույթների համար մենք եզրակացնում ենք, որ միջին և մեծ զանգվածով YSO-ի շուրջ, էվոլյուցիայի որոշակի փուլում, ձևավորվում է երիտասարդ աստղերի խումբ և փոփոխելով ընտրության չափանիշները

(լուսաչափական սահմանի խորությունը, ավելի երկար ալիքային տիրույթ)՝ հայտնաբերված խմբերի տոկոսային քանակը պետք ավելանա;

- Ընտրված YSO-ները անհամասեռ են բաշխված IRAS05137+3919 աստղառաջացման տիրույթում և կազմում են երկու ենթախումբ;
- IRAS05168+3634 տիրույթում աստղերի բաշխումը հնարավորություն տվեց հայտնաբերել հինգ խիտ ենթախմբեր IRAS աղբյուրների շուրջ, որոնք կրկնում է հեռու ինֆրակարմիր ալիքի երկարություններում դիտվող մոլեկուլային ամպի ձևը: Մենք եզրակացրինք, որ IRAS05168+3634 և այլ չորս ենթատիրույթները (IRAS 05184+3635, 05177+3636, 05162+3639, և 05156+3643) ընկղմված են մեկ ընդհանուր մոլեկուլային ամպի մեջ և *Gaia* EDR3 պարալաքսների հիման վրա գտնվում են 1.9 կպսկ հեռավորության վրա;
- IRAS05137+3919 և IRAS05168+3634 աստղառաջացման տիրույթների տարիքի բաշխումը շատ ավելի մեծ է, և, հետևաբար, կարելի է եզրակացնել, որ աստղային բնակչությունը ձևավորվել է մայր մոլեկուլային ամպի անկախ խտացումների արդյունքում;
- Մենք ենթադրում ենք, որ ցածր խտության տարածված ճառագայթումը, որը դիտվում է միջին ինֆրակարմիր տիրույթում ստացված պատկերների վրա, ինչը լավ աչքի է ընկնում նաև G45.12+0.13 և G45.07+0.13 UCHII տիրույթների T_d քարտեզներում, կարող է պայմանավորված լինել աստղակույտերի առկայությամբ;
- G45.12+0.13 և G45.07+0.13 UCHII տիրույթներում աստղակույտերի անդամները իզոխրոնների նկատմամբ ունեն փոքր ցրում, և նրանց էվոլյուցիոն տարիքի բաշխումը ցույց է տալիս փոքր տարածվածություն: Հետևաբար, մենք եզրակացնում ենք, որ դրանց ծագումը կարող է կապված լինել արտաքին հրահրող ուժի հետ;
- Ուսումնասիրված աստղառաջացման տիրույթներից միայն IRAS19110+1045 և 19111+1048 տիրույթներում են հայտնաբերվել մեծ զանգվածով աստղեր, որտեղ հավանաբար աստղառաջացման պրոցեսը հրահրվել է;
- Մենք ենթադրում ենք, որ IRAS 19110+1045 և 19111+1048 աստղակուտերից դուրս գտնվող YSO-ները հանդիսանում են GRSMC45.46+0.05 մոլեկուլային ամպի երիտասարդ աստղային բնակչության մի մասը;
- Ընտրված YSO-ների բաշխումը դաշտում ցույց տվեց, որ I դասի (Class I) օբյեկտները հիմնականում կոնցենտրացված են հայտաբերված աստղակույտերում, մինչդեռ II դասի (Class II) օբյեկտները ավելի համասեռ են բաշխված: Սա հաստատում է այն ենթադրությունը, որ ի տարբերություն Class II օբյեկտների, Class I օբյեկտները բավարար ժամանակ չեն ունեցել ձևավորվելուց հետո լքելու իրենց ծննդավայրը:

ПОИСК И ИЗУЧЕНИЕ МОЛОДЫХ ИНФРАКРАСНЫХ ЗВЕЗДНЫХ СКОПЛЕНИЙ

РЕЗЮМЕ

Диссертация посвящена исследованию областей звездообразования на основе анализа большого количества инфракрасных данных. В частности, ее основными задачами являются:

- Поиск молодых звездных скоплений в окрестностях IRAS объектов, которые, по-видимому, связаны с массивными молодыми звездными объектами (YSO);
- Идентификация членов скоплений по их свойствам в инфракрасном диапазоне;
- Исследование структурных свойств молодых звездных скоплений;
- Определение возраста и возрастного разброса членов скоплений;
- Построение функций светимости (LF) и функций масс (MF) для скоплений;
- Определение параметров межзвездной среды (ISM), а именно распределения плотности столбца водорода ($N(H_2)$) и температуры пыли (T_d).

В диссертации представлены результаты поиска и изучения звездных скоплений около 20 IRAS источников. Также представлено подробное исследование трех областей звездообразования, а именно IRAS 05137+3919, 05168+3634 и 19110+1045, которое включает изучение как звездного населения, так и ISM. Основными критериями отбора этих трех областей являются их значительная протяженность и многокомпонентная сложная структура, предполагающая наличие нескольких локальных очагов звездообразования. Эти области звездообразования представляют интерес еще и потому, что они расположены на больших расстояниях, что позволит протестировать возможности используемых нами баз данных. Результаты показывают прямую зависимость между звездной плотностью и плотностью среды во всех трех областях звездообразования. Вот основные результаты:

- Молодые компактные скопления обнаружены в окрестностях 16 из 20 IRAS источников, в том числе в 4-х - впервые. Это составляет 80% от общего числа исследованных регионов и существенно превышает результаты, полученные на данных 2MASS обзора;
- По крайней мере, для 20 областей мы пришли к выводу, что вокруг YSO средней и большой массы на определенном этапе эволюции сформировалась группа молодых звезд и при измененных критериях отбора

(глубина изображений, более длинный диапазон длин волн) процент обнаруженных групп должно увеличиться;

- Выбранные YSO неравномерно распределены в области звездообразования IRAS05137+3919 и образуют две подгруппы;
- Распределение звезд в поле IRAS05168+3634 позволило выделить пять плотных подгрупп вокруг источников IRAS, повторяющих форму молекулярного облака, наблюдаемого в дальнем инфракрасном диапазоне. Мы пришли к выводу, что IRAS05168+3634 и другие четыре подобласти (IRAS 05184+3635, 05177+3636, 05162+3639 и 05156+3643) встроены в единое молекулярное облако и на основе параллаксов *Gaia* EDR3 расположены на расстоянии ~1.9 кпк;
- Разброс возрастов областей звездообразования IRAS05137+3919 и IRAS05168+3634 значительно больше, поэтому можно сделать вывод, что звездное население формируется в результате самостоятельных конденсаций в родительском молекулярном облаке;
- Мы предполагаем, что расширенное излучение низкой плотности наблюдаемое на изображениях среднего инфракрасного диапазона, которое также хорошо выделяется на картах температуры пыли в областях G45.12+0.13 и G45.07+0.13 UCHII, может быть связано с существованием звездных скоплений;
- Члены скоплений IRAS в областях G45.12+0.13 и G45.07+0.13 UCHII имеют небольшой разброс относительно изохрон, и их эволюционное возрастное распределение показывает небольшой разброс. Поэтому мы делаем вывод, что их происхождение может быть связано с внешним триггерным шоком.
- Среди рассмотренных областей звездообразования массивные звезды были обнаружены только в области, где, по всей видимости, звездообразование было инициировано внешним триггерным шоком, то есть IRAS19110+1045 и 19111+1048;
- Мы предполагаем, что YSO вне скоплений IRAS 19110+1045 и 19111+1048 являются частью молодого звездного населения молекулярного облака GRSMC45.46+0.05;
- Распределение выбранных YSO в поле показало, что объекты класса I (Class I) в основном расположены в обнаруженных звездных скоплениях, а объекты класса II (Class II) распределены более равномерно в поле молекулярного облака. Это подтверждает предположение, что, в отличие от объектов Class II, объекты Class I не успели покинуть место своего рождения после формирования.

Նաիրա Ազատյան / Naira Azatyan / Наира Азатян _____